

Supplementary Materials

for

Discovery and characterization of amentoflavone as a naturally occurring inhibitor against the bile salt hydrolase produced by *Lactobacillus salivarius*

Chun-Yu Li^{a,1}, Hao-Nan Wang^{a,1}, Rong-Jing He^a, Jian Huang^{a,b}, Li-Lin Song^c, Yun-Qing
Song^a, Peng-Chao Huo^a, Jie Hou^d, Guang Ji^{e,*}, Guang-Bo Ge^{a,*}

^a Shanghai Frontiers Science Center for Chinese Medicine Chemical Biology; Institute of Interdisciplinary Integrative Medicine Research, Shanghai University of Traditional Chinese Medicine, 1200 Cailun Road, Shanghai 201203, China.

^b Pharmacology and Toxicology Division, Shanghai Institute of Food and Drug Control, Shanghai 201203, China.

^c Dalian Institute of Chemical Physics, Chinese Academy of Sciences, Dalian 116000, China.

^d College of Basic Medical Sciences, Dalian Medical University, Dalian, 116044, China.

^e Institute of Digestive Disease, Longhua Hospital, Shanghai University of Traditional Chinese Medicine, Shanghai 200032, China.

*Corresponding author.

E-mail address: geguangbo@dicp.ac.cn (G.B. Ge); jliver@vip.sin (G. Ji)

¹ Contributed equally.

This file contains two supplementary tables and thirteen supplementary figures.

Table S2. The results of CavityPlus calculation. 5y7p

No.	Pred.Avg pKd	Druggability
1	6.94	Strong
2	6.66	Medium

Pred.Avg pKd: The average value indicates the ligandability of a cavity binding site. A value less than 6.0 suggests that this site may not be a suitable ligand-binding site. Druggability indicates the possibility of a cavity binding site to be druggable or not.

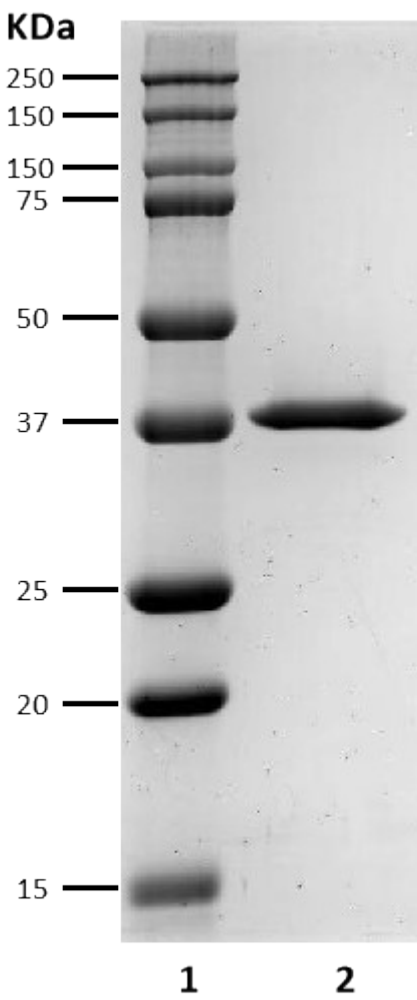


Fig. S1 SDS-PAGE analysis of the purification of lsBSH. (1. Marker; 2. Purified on a Superdex 200 10/300 GL column).

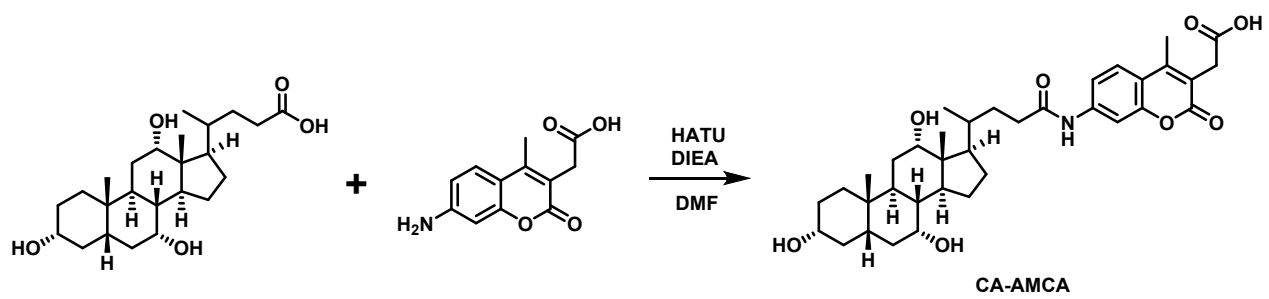


Fig S2 The synthetic procedure of CA-AMCA.

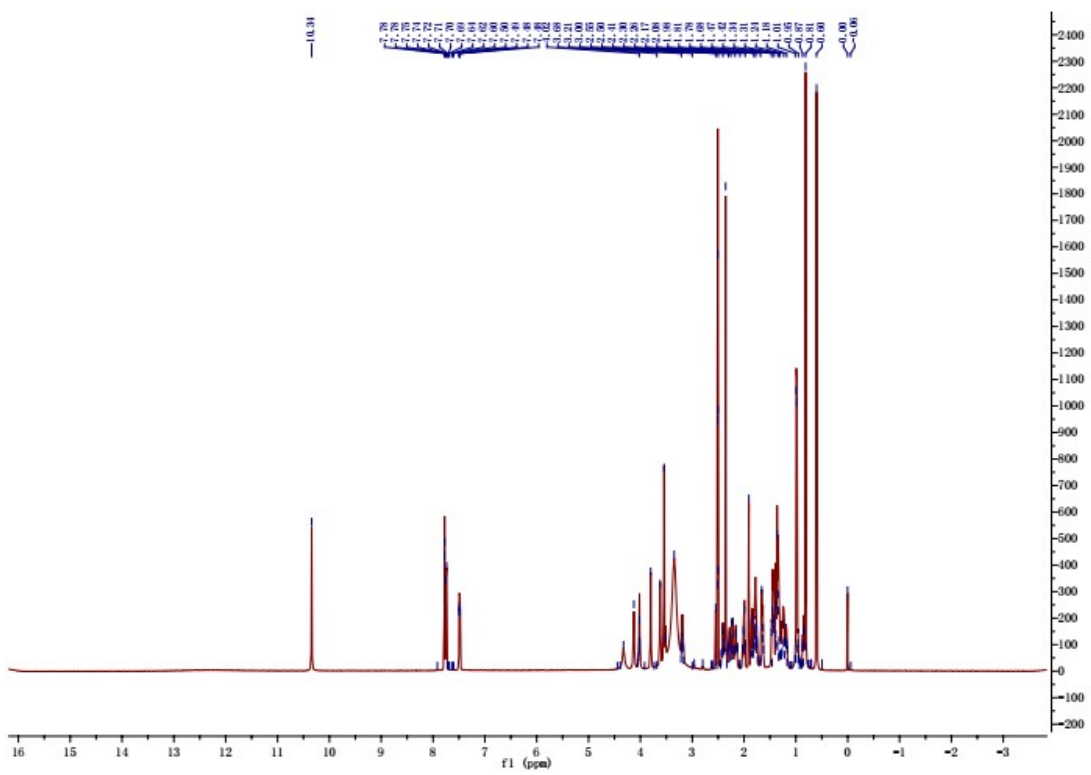


Fig.S3 ^1H NMR (500 MHz, CDCl_3) spectrum of CA-AMCA.

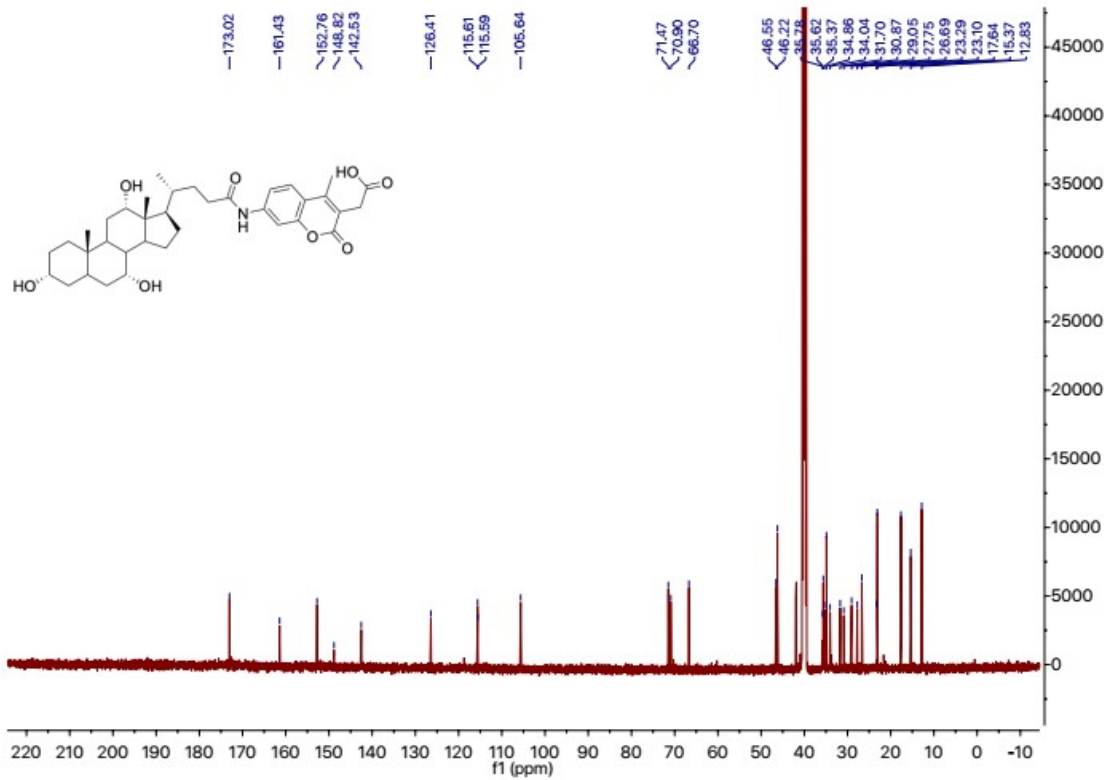
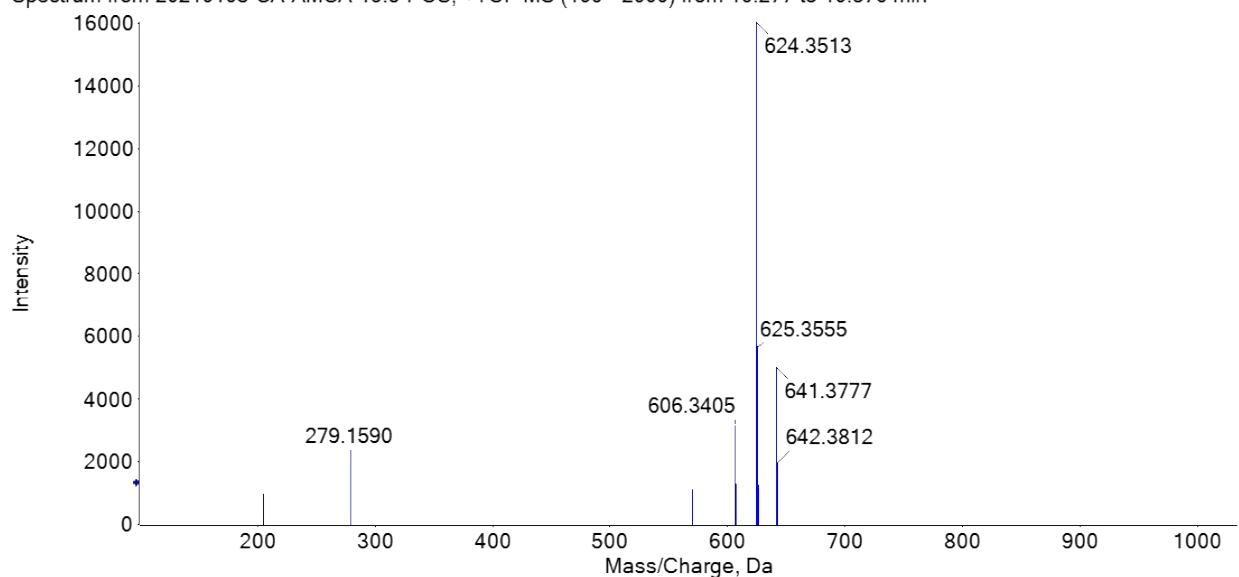


Fig.S4 ^{13}C NMR (125 MHz, DMSO-d_6) spectrum of CA-AMCA.

A Spectrum from 20210108-CA-AMCA-19.5-POS, +TOF MS (100 - 2000) from 10.277 to 10.376 min



B Spectrum from 20210108-CA-AMCA-19.5-POS, +TOF MS² (100 - 2000) from 10.305 min
Precursor: 624.4 Da, CE: 35.0

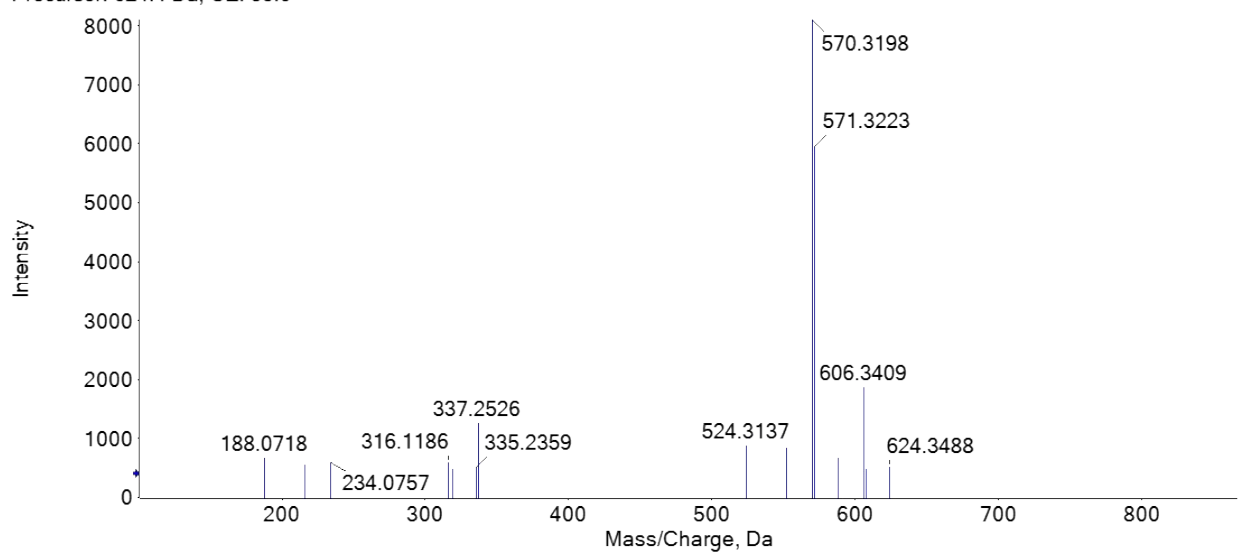


Fig. S5 MS¹ (A) and MS² (B) spectra of CA-AMCA.

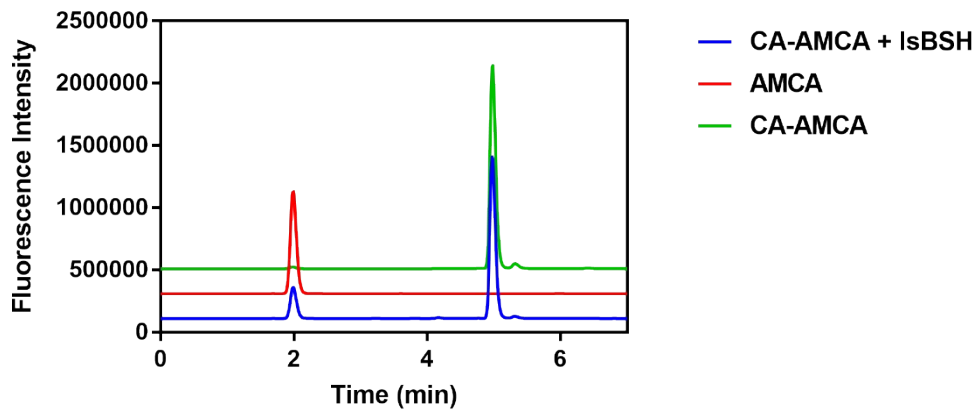


Fig. S6 Liquid chromatography-fluorescence detection (LC-FD) chromatograms of AMCA and CA-AMCA. (Green) CA-AMCA only, (Red) AMCA only, (Blue) CA-AMCA was co-incubated with lsBSH (2 µg/mL) at 37 °C for 30 min. The fluorescence signals of AMCA and CA-AMCA were recorded using excitation wavelength of 345 nm and emission wavelength of 455 nm.

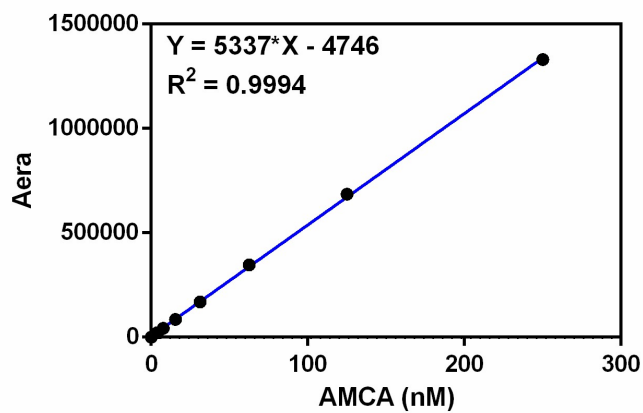


Fig. S7 The standard curve of AMCA (the hydrolytic metabolite of CA-AMCA).

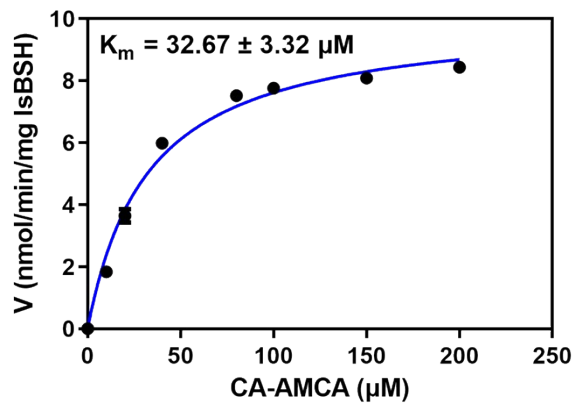


Fig. S8 Enzymatic kinetic plot of lsBSH-catalyzed CA-AMCA hydrolysis.

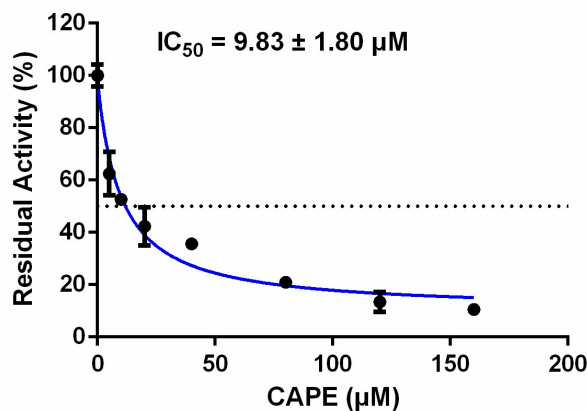


Fig. S9 The dose-inhibition curve of CAPE against lsBSH-catalyzed CA-AMCA hydrolysis.

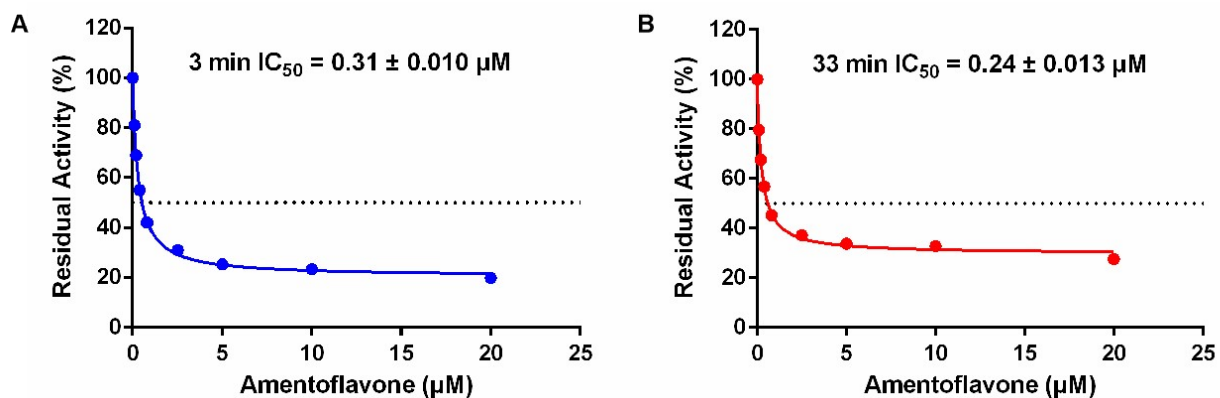


Fig. S10 The residual activity of lsBSH-catalyzed CA-AMCA hydrolysis in the presence of different concentrations of AMF at different pre-incubation times of 3 minutes (A) and 33 minutes (B). All data were shown as mean ± SD of triplicate determinations.

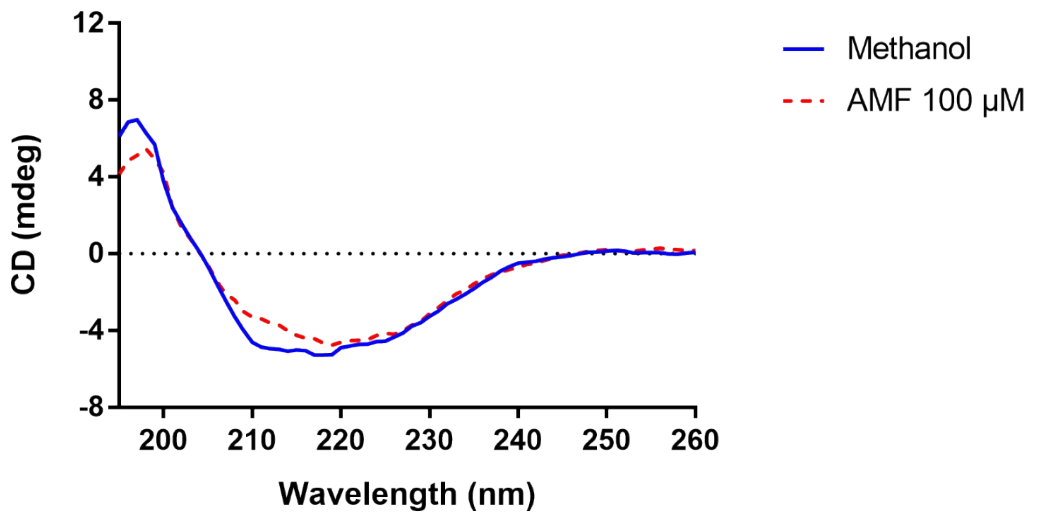


Fig. S11 Circular dichroism spectra of lsBSH and lsBSH-AMF complex.

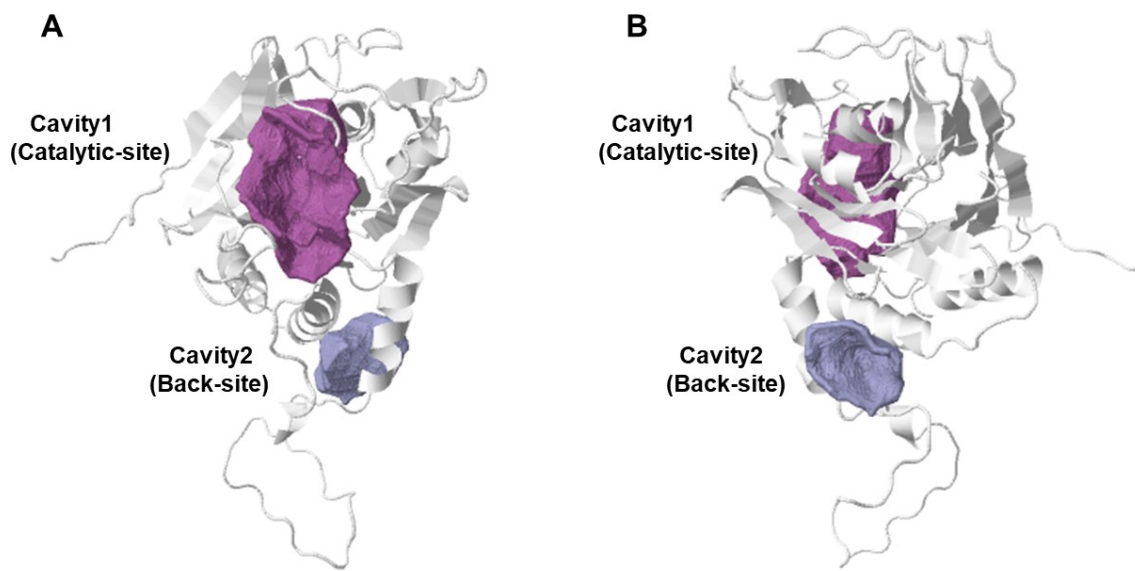


Fig. S12 Two possible ligand-binding pockets were predicted with CavityPlus. (A) Front view, (B) Back view.

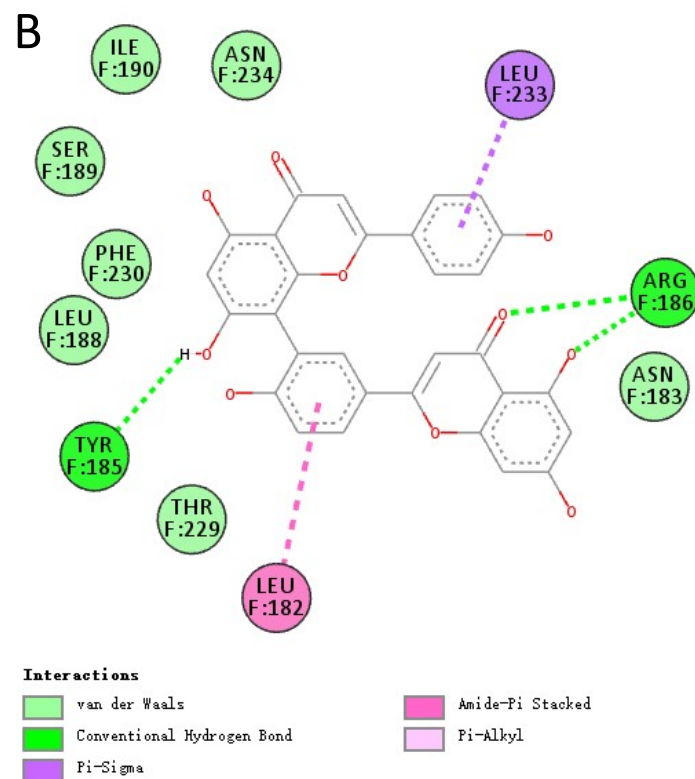
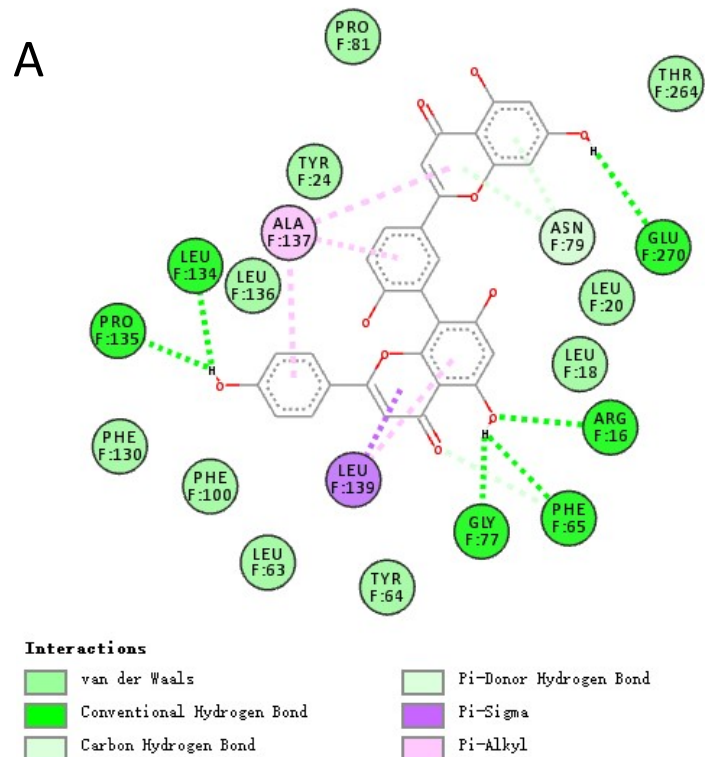


Fig. S13 2D interactions of AMF with lsBSH in the catalytic site (A) and back site (B).